

to respond to the forces exerted on them. By phase-space considerations (very thin oxide), $a \approx 1$, and during this interval the Schottky relation (1) holds approximately.

What happens now for $t \gg t_1$ [Fig. 1(c)] depends on the relative lattice rigidities of the oxide and the semiconductor. Again $\Delta\phi$ is separated into two parts, $S\Delta\phi$ being added to ϕ_B and $(1-S)\Delta\phi$ being described by an oxide dielectric double layer. If the oxide is more stable [as is the case when $\omega_g(MX) < \omega_s < \tilde{\omega}_g(MO)$ described by Eq. (5)], near the interface the semiconductor ions will be displaced quasielastically in such a way as to eject the accumulated charge described by surface plasmons into the oxide. This gives the Bardeen limit $S(s) \approx 0$. On the other hand, if the semiconductor is so ionic itself as to be more stable than the $M'O$ oxide, then the latter ejects its share of the interfacial charge into the semiconductor, and the Schottky limit $S(s) \approx 1$ holds. The deformation mechanism proposed here is

¹¹ J. C. Phillips, Phys. Rev. Letters **22**, 285 (1969).

related to the cancellation theorem¹¹ for substitutional isoelectronic impurities, where a similar charge accumulation and ejection occurs because of electronegativity differences.

Because of the quasielastic deformation associated with charge ejection in the Bardeen limit, the mathematics of surface states at ideal interfaces⁷ may not be quite relevant to barrier heights in this limit. There one would expect elastic mismatch to account for the small barrier heights (of order a few tenths of an eV) that are actually observed. Because lattice distortions are of longer range, one might expect that for a family of elastically similar semiconductors the resulting barrier could be related to properties of the valence and conduction band edges only (rather than the average gap E_g). Thus it is not surprising that for many covalent semiconductors¹² (Bardeen limit) $\phi_B \approx \phi_{Be} \approx 0.3\Delta E_{cv}$, where ΔE_{cv} denotes the minimum (direct or indirect) gap between valence- and conduction-band edges.

¹² C. A. Mead and W. G. Spitzer, Phys. Rev. **134**, A173 (1964).

Lattice Dynamics of Wurtzite: CdS. II[†]

MICHEL A. NUSIMOVICI*[‡] AND MINKO BALKANSKI

*Laboratoire de Physique des Solides de la Faculté des Sciences de Paris, France,
Équipe de Recherche associée au Centre National de la Recherche Scientifique*

AND

JOSEPH L. BIRMAN*

Physics Department, New York University, New York, New York

(Received 19 May 1969)

A new model for the lattice dynamics of semi-ionic compounds is presented and applied to the computation of phonon dispersion in CdS. The calculated two-phonon density of states as a function of frequency is in agreement with measured infrared absorption in the two-phonon region. Improved values of the microscopic dielectric, elastic, and piezoelectric coefficients result from a self-consistent least-squares fit of model parameters. The model includes valence-band forces, rigid-ion Coulomb forces, and electronic and ionic polarization; it may be generally applicable to other semi-ionic II-VI compounds.

I. INTRODUCTION

THE present paper reports on an improved model developed for the lattice dynamics of II-VI partially ionic compounds. The improved model is based upon the mixed valence-Coulomb force field model previously used¹ to calculate phonon dispersion in CdS; however, the ionic polarization and the ion deformation

(electronic polarizabilities) are now included in the model, which thereby incorporates most of the likely important basic physical phenomena involved.

As previously noted,¹ only indirect checks of the calculated CdS phonon frequencies are possible, since no experimental inelastic neutron scattering spectra have been reported in CdS from which the dispersion curves can be obtained. We find improved agreement of calculated two-phonon density of modes and two-phonon infrared absorption spectra in the spectral region 400 to 600 cm^{-1} ; major features agree to within 5 cm^{-1} . The elastic and piezoelectric constants of CdS have also been calculated, and the difference with ex-

[†] This paper is based in part on the thesis presented to the Faculté des Sciences, University of Paris, Paris, France, for the degree Docteur-ès-Sciences Physiques, 1968, by Michel A. Nusimovici.

* Supported in part by the Aerospace Research Laboratories, Wright-Patterson Air Force Base, Dayton, Ohio, and the U. S. Army Research Office, Durham, N. C.

[‡] Present address: Faculté des Sciences, 35-Rennes Beaulieu, France.

¹ M. A. Nusimovici and J. L. Birman, Phys. Rev. **156**, 925 (1967).

perimental values is smaller than 8%; this also represents an improvement over our previous results² based on the model which omitted the polarizabilities.

We have applied our calculated results in perfect CdS to the determination of phonon frequencies of CdS containing mass defects. The results are reported in an accompanying paper,³ which improves upon the preliminary results already given.⁴

A calculation of phonon frequencies is in progress using the present improved model for BeO. While at present only partial neutron scattering results are available in BeO,⁵ there is hope that all branches of the phonon spectrum can be determined. The results of the calculation, and a direct comparison with an experiment to test the model will be reported elsewhere.⁵

II. THEORY

It will be assumed that the reader is conversant with the work reported in a previous paper¹ (I) to which liberal reference will be made in the interest of brevity. The first step in the work involves the construction of the dynamical matrix. This necessitates specifying the forces and force constants characterizing the problem.

Valence Forces

The short-range valence force parts of the potential energy are taken over from the previous work, with additions. As discussed there, this implies inclusion of all interactions of a given ion with neighbors up to and including third neighbor. From I (3.9), we see that there are eight spring constants to be determined, including radial, angular, and cross coupling constants. In addition, we considered in the present work the constants k_{rr} and $k_{rr'}$ corresponding to three-body quadrupolar forces due to a short-range deformation of the electronic orbitals; ten spring constants have then to be determined, which can be reduced to eight if one considers that the Cd ion is heavy and small and hence assumes that the three-body S-Cd-S constants vanish. The three-body Cd-S-Cd constants are nonzero.

Coulomb Forces

The previous treatment of Coulomb forces assumed the ions were point (undeformable) ions with fixed charges. This corresponds to taking the dipole moment arising at site $(0,\kappa)$ as

$$\mathbf{p}' = q_\kappa \mathbf{u}(0,\kappa), \quad (2.1)$$

² M. A. Nusimovici and J. L. Birman, in *Proceeding of the International Conference on II-VI Semiconducting Compounds, New York, 1967*, edited by D. G. Thomas (W. A. Benjamin, Inc., New York, 1967), p. 1204.

³ M. A. Nusimovici, M. Balkanski, and J. L. Birman, following paper, *Phys. Rev. B* **1**, 603 (1969).

⁴ P. Pfeuty, J. L. Birman, M. A. Nusimovici, and M. Balkanski, in *Proceedings of the International Conference on Localized Excitations in Solids, Irvine, Calif., 1967*, edited by R. Wallis (Plenum Press, Inc., New York, 1968), p. 210.

⁵ M. A. Nusimovici, *Compt. Rend.* **268**, 755 (1969).

where $\mathbf{u}(0,\kappa)$ is the displacement of the ion initially at $(0,\kappa)$, and q_κ a static charge.

Now, let α_κ be the scalar polarizability of the κ th ion. Then if \mathbf{E} is the local electric field acting on that ion, the moment

$$\mathbf{p}'' = \alpha_\kappa \mathbf{E}(0,\kappa) \quad (2.2)$$

will be associated with ion $(0,\kappa)$.

In a central first-neighbor approximation, we can define a deformation dipole moment (and a parameter γ_κ having formal dimension of a charge) corresponding to ionic charge deformation linearly dependent on the relative ionic displacement. This will produce a local dipole moment

$$\mathbf{p}''' = \gamma_\kappa \sum_{\kappa',\nu'} \frac{\mathbf{r}(0l,\kappa\kappa') \cdot \mathbf{r}(0l,\kappa\kappa')}{r_0^2} [\mathbf{u}(0,\kappa) - \mathbf{u}(0,\kappa')]. \quad (2.3)$$

The sum in (2.3) extends over the four ions (l,κ') which are first neighbors of the ion (l,κ) , and $\mathbf{r}(0l,\kappa\kappa')$ is the vector from ion $(0,\kappa)$ to ion (l,κ') .

The total dipole moment of ion $(0,\kappa)$ arising during the vibration is then

$$\mathbf{P}_\kappa = q_\kappa \mathbf{u}(0,\kappa) + \alpha_\kappa \mathbf{E}_\kappa + \gamma_\kappa \sum_{\kappa',\nu'} \frac{\mathbf{r}(0l,\kappa\kappa') \cdot \mathbf{r}(0l,\kappa\kappa')}{r_0^2} [\mathbf{u}(0,\kappa) - \mathbf{u}(0,\kappa')]. \quad (2.4)$$

In what follows we choose

$$\gamma_{ca} = 0, \quad \gamma_s = \gamma. \quad (2.5)$$

The justification of (2.5), besides convenience, is that the small size and heavy mass of Cd should result in a small deformation dipole. It is convenient to write (2.1)–(2.4) in matrix notation. Thus, let \mathbf{U} be a column matrix with 12 rows composed from the displacements $\mathbf{u}(0,\kappa)$ and let \mathbf{Q} , α and $\mathbf{N}(\boldsymbol{\eta})$ be 12×12 square matrices defined by

$$\mathbf{Q}_{\kappa\kappa'} = q_\kappa \delta_{\kappa\kappa'} \mathbf{I}_3, \quad (2.6)$$

$$\alpha_{\kappa\kappa'} = \alpha_\kappa \delta_{\kappa\kappa'} \mathbf{I}_3, \quad (2.7)$$

$$\mathbf{N}(\boldsymbol{\eta})_{\kappa\kappa'} = \gamma_\kappa \sum_{\nu'} \frac{\mathbf{r}(0l,\kappa\kappa') \cdot \mathbf{r}(0l,\kappa\kappa')}{r_0^2}. \quad (2.8)$$

In Eqs. (2.6) and (2.7), \mathbf{I}_3 is the unit 3×3 matrix. The sum in (2.8) is extended over all cells with ions (l,κ') which are first neighbors of the ion $(0,\kappa)$. Call \mathbf{E} a 12-rowed column vector each component of which gives a Cartesian component α of the local electric field \mathbf{E}_κ at the site of the κ ion. Then instead of (2.4) we write

$$\mathbf{P} = [\mathbf{Q} + \mathbf{N}(\boldsymbol{\eta})] \cdot \mathbf{U} + \alpha \cdot \mathbf{E}. \quad (2.9)$$

A lattice of vibrating point dipoles produces a local electric field given by

$$\mathbf{E}_\kappa = \sum_{\kappa'} \mathbf{B}(\boldsymbol{\eta})_{\kappa\kappa'} \cdot \mathbf{p}_{\kappa'}, \quad (2.10)$$

where $\mathbf{B}(\boldsymbol{\eta})_{\kappa\kappa'}$ is the "Lorentz matrix" given by I (3.19). Hence we may write

$$\mathbf{P} = [\mathbf{I} - \boldsymbol{\alpha} \cdot \mathbf{B}(\boldsymbol{\eta})]^{-1} \cdot [\mathbf{Q} + \mathbf{N}(\boldsymbol{\eta})] \cdot \mathbf{U}, \quad (2.11)$$

or

$$\mathbf{P} = [\mathbf{I} - \boldsymbol{\alpha} \cdot \mathbf{B}(\boldsymbol{\eta})]^{-1} \cdot [\mathbf{Q} + \mathbf{N}(\boldsymbol{\eta})] \cdot \mathbf{U}, \quad (2.12)$$

which gives a linear relationship between the displacements and the dipole moments. Finally, from (2.10) and (2.12)

$$\mathbf{E} = \mathbf{B}(\boldsymbol{\eta}) \cdot [\mathbf{I} - \boldsymbol{\alpha} \cdot \mathbf{B}(\boldsymbol{\eta})]^{-1} \cdot [\mathbf{Q} + \mathbf{N}(\boldsymbol{\eta})] \cdot \mathbf{U}. \quad (2.13)$$

Dynamical Matrix

As in our previous work, we calculate the complete 12-dimensional square matrix as the sum of a valence-force dynamical matrix which is obtained as the second derivative of the potential (I) (3.9) with respect to ion-position coordinates plus the Coulomb-force dynamical matrix. The former contribution was already discussed in the previous work (I).

To obtain the Coulomb-force dynamical matrix, we require an expression for the potential energy of the system of vibrating dipoles in the presence of the time-varying electric field associated with the lattice vibration. This can be written as

$$V^c = \mathbf{P}^* \cdot \mathbf{E} = \sum_{\kappa=1}^4 \sum_{\kappa'=1}^3 (\mathbf{p}_{\kappa})_{\alpha} (\mathbf{E}_{\kappa})_{\alpha}. \quad (2.14)$$

Differentiating (2.4) twice with respect to displacements $\mathbf{u}(0, \kappa)$, we obtain the Coulomb part of the dynamical matrix which can be written in an obvious notation as

$$\mathbf{C}(\boldsymbol{\eta})_{\text{Coul}} = \mathbf{M}^{-1/2} \cdot [\mathbf{Q} + \mathbf{N}(\boldsymbol{\eta})] \cdot \mathbf{B}(\boldsymbol{\eta}) \cdot [\mathbf{I} - \boldsymbol{\alpha} \cdot \mathbf{B}(\boldsymbol{\eta})]^{-1} \cdot [\mathbf{Q} + \mathbf{N}(\boldsymbol{\eta})] \cdot \mathbf{M}^{-1/2}. \quad (2.15)$$

In Eq. (2.15), $\mathbf{N}(\boldsymbol{\eta})$ is the transpose of $\mathbf{N}(\boldsymbol{\eta})$. \mathbf{M} is a matrix defined by

$$(\mathbf{M})_{\kappa\kappa'} = M_{\kappa} \cdot \delta_{\kappa\kappa'}. \quad (2.16)$$

We verify that $\mathbf{C}(\boldsymbol{\eta})$ is Hermitian by showing $\mathbf{B} \cdot (\mathbf{I} - \boldsymbol{\alpha} \cdot \mathbf{B})^{-1}$ is Hermitian. This matrix can be transformed as

$$\mathbf{B} \cdot (\mathbf{I} - \boldsymbol{\alpha} \cdot \mathbf{B})^{-1} = (\mathbf{B}^{-1} - \boldsymbol{\alpha})^{-1}. \quad (2.17)$$

Now, \mathbf{B} being Hermitian, so is \mathbf{B}^{-1} . Therefore $(\mathbf{B}^{-1} - \boldsymbol{\alpha})$ and $(\mathbf{B}^{-1} - \boldsymbol{\alpha})^{-1}$ are Hermitian; hence, so is $\mathbf{C}(\boldsymbol{\eta})$.

Long-Wave-Limit Eigenfrequencies

In the long wave limit $|\eta| \rightarrow 0$, the secular equation for the eigenfrequencies of the dynamical matrix factorizes, and we may obtain explicit expressions for the squares of the eigenfrequencies in terms of the parameters of the model. We shall merely describe the factorization which is straightforward and give the results. Additional details are given in Ref. 6. Notice

⁶ M. A. Nusimovici, thèse, Faculté des Sciences de l'Université de Paris, 1968 (unpublished).

that the valence and Coulomb contributions to the dynamical matrix may be separately obtained in the $\boldsymbol{\eta} \rightarrow 0$ limit. The Coulomb contribution [especially the Lorentz matrix $\mathbf{B}(\boldsymbol{\eta})$] is not analytic at $\boldsymbol{\eta} = 0$, but depends on the direction of approach of zero wave vector. Also, as discussed previously by Kaplan and Sullivan,⁷ one may easily obtain "additive" and "subtractive" modes of vibration; in the former, the two identical ions in the cell (e.g., Cd) move in phase, in the latter, out of phase. It can be shown that in case of the additive modes, the effect of including the deformation dipole contribution (2.3) is to renormalize the effective charge from q to

$$q^* = q - \frac{4}{3}\gamma. \quad (2.18)$$

This is equivalent to introducing the Szigetti's effective charge q^* into the rigid-ion model.⁸ For the additive Γ_5 optical modes in parallel polarization, using the Clausius-Mosotti equations, one obtains a transverse charge

$$q_t = \frac{1}{3}(\epsilon_{\infty} + 2)q^*, \quad (2.19)$$

while for the longitudinal Γ_1 optical mode, a longitudinal charge

$$q_l = q_t / \epsilon_{\infty} = q^*(\epsilon_{\infty} + 2) / 3\epsilon_{\infty} \quad (2.20)$$

is appropriate with

$$3/q^* = 2/q_t + 1/q_l. \quad (2.21)$$

In the rigid-ion model, both longitudinal and transverse charges are equal:

$$q_t = q_l. \quad (2.22)$$

Now we give the results of the $\boldsymbol{\eta} \rightarrow 0$ factorization for the eigenfrequencies. Results will be given in terms of a rotation for the matrix elements of the four 3×3 submatrices comprising the dynamical matrix. Further details are given in Ref. 1.

$$\boldsymbol{\eta} \rightarrow 0 \parallel Z$$

$$\omega^2(\Gamma_5) = R_{11} + S_{11} + E_{11} + F_{11} + \sigma_1 q^* q_t (M_S + M_{Cd} / M_S M_{Cd}), \quad (2.23)$$

$$\omega^2(\Gamma_1) = R_{33} + S_{33} + E_{33} + F_{33} - (2\sigma_1 q^* q_t / \epsilon_{\infty}) (M_S + M_{Cd} / M_S M_{Cd}); \quad (2.24)$$

$$\boldsymbol{\eta} \rightarrow 0 \parallel X$$

$$\omega^2(\Sigma_1, \text{LO}) = R_{11} + S_{11} + E_{11} + F_{11} + [\sigma_1' q^{*2} / 1 - \sigma_1' (\alpha_{Cd} + \alpha_S)] \times (M_S + M_{Cd} / M_S M_{Cd}), \quad (2.25)$$

$$\omega^2(\Sigma_1, \text{TO}) = R_{33} + S_{33} + E_{33} + F_{33} + [\sigma_3' q^{*2} / 1 - \sigma_3' (\alpha_{Cd} + \alpha_S)] \times (M_S + M_{Cd} / M_S M_{Cd}); \quad (2.26)$$

⁷ H. Kaplan and J. Sullivan, Phys. Rev. **130**, 120 (1963).

⁸ B. Szigeti, Proc. Roy. Soc. (London) **A204**, 51 (1950).

$\eta \rightarrow 0$ (arbitrary polarization)

$$\omega^2(\Gamma_6) + \omega'^2(\Gamma_6) = R_{11} + E_{11} - S_{11} - F_{11} + X_1/M_{\text{Cd}} + Z_1/M_{\text{S}}, \quad (2.27)$$

$$\begin{aligned} \omega^2(\Gamma_6) \cdot \omega'^2(\Gamma_6) &= (R_{11} - S_{11} + X_1/M_{\text{Cd}})(E_{11} - F_{11} + Z_1/M_{\text{S}}) \\ &\quad - (T_{11} - U_{11} + Y_1/M_{\text{S}}M_{\text{Cd}})^2, \end{aligned} \quad (2.28)$$

$$\omega^2(\Gamma_4) + \omega'^2(\Gamma_4) = R_{33} + E_{33} - S_{33} - F_{33} + (X_3/M_{\text{Cd}} + Z_3/M_{\text{S}}), \quad (2.29)$$

$$\begin{aligned} \omega^2(\Gamma_4) \cdot \omega'^2(\Gamma_4) &= (R_{33} - S_{33} + X_3/M_{\text{Cd}})(E_{33} - F_{33} + Z_3/M_{\text{S}}) \\ &\quad - (T_{33} - U_{33} + Y_3/M_{\text{S}}M_{\text{Cd}})^2. \end{aligned} \quad (2.30)$$

The quantities R_{ii} , S_{ii} , T_{ii} , U_{ii} , E_{ii} , and F_{ii} ($i=1, 2$, or 3) appearing in Eqs. (2.23)–(2.30) correspond to the short-range-forces contributions, and they are defined by

$$\begin{aligned} R_{11} = & \left[\frac{4}{3}\lambda + \mu + k_\theta + (16/3)(k_\theta + k_{\theta'}) \right. \\ & + 2\sqrt{2}k_r + (16\sqrt{2}/3)(k_{r\theta} + k_{r\theta'}) \\ & \left. - \frac{4}{3}(k_{rr} + k_{rr'}) \right] \times 1/M_{\text{Cd}}, \end{aligned} \quad (2.31)$$

$$\begin{aligned} R_{33} = & \left[\frac{4}{3}\lambda + 4\mu + (16/3)(k_\theta + k_{\theta'}) \right. \\ & + 4\sqrt{2}k_{r\theta} + (16\sqrt{2}/3)(k_{r\theta} + k_{r\theta'}) \\ & \left. - 2k_{rr} - \frac{4}{3}(k_{rr} + k_{rr'}) \right] \times 1/M_{\text{Cd}}, \end{aligned} \quad (2.32)$$

$$S_{11} = M_{\text{Cd}}^{-1}(-\mu - k_\theta - 2\sqrt{2}k_{r\theta}), \quad (2.33)$$

$$S_{33} = M_{\text{Cd}}^{-1}(-4\mu + 2k_{rr}), \quad (2.34)$$

$$T_{11} = (M_{\text{S}}M_{\text{Cd}})^{-1/2}[-2(k_\theta + k_{\theta'}) - \sqrt{2}(k_{r\theta} + k_{r\theta'})], \quad (2.35)$$

$$\begin{aligned} T_{33} = & (M_{\text{S}}M_{\text{Cd}})^{-1/2}[-\lambda - \delta - 2\sqrt{2}(k_{r\theta} + k_{r\theta'}) \\ & + (k_{rr} + k_{rr'})], \end{aligned} \quad (2.36)$$

$$\begin{aligned} U_{11} = & (M_{\text{S}}M_{\text{Cd}})^{-1/2}[-\frac{4}{3}\lambda - (10/3)(k_\theta + k_{\theta'}) \\ & + \frac{4}{3}(k_{rr} + k_{rr'}) - (13\sqrt{2}/3)(k_{r\theta} + k_{r\theta'})], \end{aligned} \quad (2.37)$$

$$\begin{aligned} U_{33} = & (M_{\text{S}}M_{\text{Cd}})^{-1/2}[-\frac{1}{3}\lambda - (16/3)(k_\theta + k_{\theta'}) \\ & + \frac{1}{3}(k_{rr} + k_{rr'}) - (10\sqrt{2}/3)(k_{r\theta} + k_{r\theta'})], \end{aligned} \quad (2.38)$$

$$\begin{aligned} E_{11} = & \left[\frac{4}{3}\lambda + \nu + k_{\theta'} + (16/3)(k_\theta + k_{\theta'}) \right. \\ & + 2\sqrt{2}k_{r\theta'} + (16\sqrt{2}/3)(k_{r\theta} + k_{r\theta'}) \\ & \left. - \frac{4}{3}(k_{rr} + k_{rr'}) \right] \times 1/M_{\text{S}}, \end{aligned} \quad (2.39)$$

$$\begin{aligned} E_{33} = & \left[\frac{4}{3}\lambda + 4\nu + (16/3)(k_\theta + k_{\theta'}) \right. \\ & + 4\sqrt{2}k_{r\theta'} + (16\sqrt{2}/3)(k_{r\theta} + k_{r\theta'}) \\ & \left. - 2k_{rr} - \frac{4}{3}(k_{rr} + k_{rr'}) \right] \times 1/M_{\text{S}}, \end{aligned} \quad (2.40)$$

$$F_{11} = M_{\text{S}}^{-1}(-\nu - k_{\theta'} - 2\sqrt{2}k_{r\theta'}), \quad (2.41)$$

$$F_{33} = M_{\text{S}}^{-1}(-4\nu + 2k_{rr'}). \quad (2.42)$$

The quantities X_i , Y_i , Z_i which correspond to the Coulomb forces are defined by

$$X_i = X_i'q^2 + w \cdot (2q \cdot Y_i' + wZ_i'), \quad (2.43)$$

$$Y_i = -qQ^*Y_i' - wq^*Z_i', \quad (2.44)$$

$$Z_i = q^{*2}Z_i', \quad (2.45)$$

with

$$X_i' = \frac{\nu_i - \alpha_{\text{S}}(\nu_i^2 - \tau_i^2)}{1 - (\alpha_{\text{S}} + \alpha_{\text{Cd}})\nu_i + \alpha_{\text{S}}\alpha_{\text{Cd}}(\nu_i^2 - \tau_i^2)}, \quad (2.46)$$

$$Y_i' = \frac{\tau_i}{1 - (\alpha_{\text{S}} + \alpha_{\text{Cd}})\nu_i + \alpha_{\text{S}}\alpha_{\text{Cd}}(\nu_i^2 - \tau_i^2)}, \quad (2.47)$$

$$Z_i' = \frac{\nu_i - \alpha_{\text{Cd}}(\nu_i^2 - \tau_i^2)}{1 - (\alpha_{\text{S}} + \alpha_{\text{Cd}})\nu_i + \alpha_{\text{S}}\alpha_{\text{Cd}}(\nu_i^2 - \tau_i^2)}. \quad (2.48)$$

The relations (2.43)–(2.45) correspond to the contribution of the deformation dipoles, and Eqs. (2.46)–(2.48) correspond to the contribution of the ionic polarizabilities. q^* is the effective charge defined by Eq. (2.18), and σ_i and σ_i' correspond to additive combinations of the elements of Lorentz matrices \mathbf{B}_1 and \mathbf{B}_2 defined by

$$\sigma_i = B_{i,i} + B_{i,i+3}, \quad (2.49)$$

$$\nu_i = B_{i,i+6} - B_{i,i+9}, \quad (2.50)$$

$$\tau_i = B_{i,i} - B_{i,i+3}, \quad (2.51)$$

where the various combination of the $\eta \rightarrow 0$ Lorentz matrix in (2.49)–(2.51) are given in the Appendix.

The modes Γ_1 , Γ_5 , $\Sigma_1(\text{LO})$, and $\Sigma_1(\text{TO})$ induce an electric dipole moment in the crystal, and the previous calculation yields a discontinuity in the center of the Brillouin zone. They are defined in the limit of a vanishing wave vector which cannot be set equal to zero.⁹ The trace of the Lorentz matrix vanishes, and therefore Eqs. (2.23)–(2.26) are dependent; the fourth one can be obtained from the three previous ones.

Long Wave Limit—Acoustic Branches

Using the long wave limit of the dynamical matrix in our model, expressions can be derived for the various macroscopic constants. Following the same procedure originated by Born and Huang,¹⁰ we split off the non-analytic part of the dynamical matrix due to the long-wave-direction-dependent part of the Coulomb field, whose asymptotic value can be found. The remaining terms in both the valence and the Coulomb part of the dynamical matrix are analytic, and they can be expanded in a power series in the wave vector. Identification of the macroscopic elastic, piezoelectric, and dielectric coefficients then easily follows: The local (effective) field can be obtained as

$$\mathbf{E}_{\text{eff}} = \mathbf{B} \cdot \mathbf{P}. \quad (2.52)$$

Let \mathbf{B}_a be the analytic part of \mathbf{B} , then $(\mathbf{B} - \mathbf{B}_a)$ is not analytic. The macroscopic field is then

$$\mathbf{E}_{\text{mac}} = (\mathbf{B} - \mathbf{B}_a) \cdot \mathbf{P}. \quad (2.53)$$

⁹ L. Merten, Z. Naturforsch **13A**, 662 (1958); **13A**, 1067 (1958); **15A**, 512 (1960); **15A**, 626 (1960); **17A**, 65 (1961); **17A**, 174 (1962); **17A**, 216 (1962).

¹⁰ M. Born and K. Huang, *Dynamical Theory of Crystal Lattices* (Oxford University Press, Oxford, 1964).

The continuous part of the electric field \mathbf{E} can be obtained as

$$\mathbf{E} = \mathbf{B}_a \cdot \mathbf{P} = \mathbf{B}_a \cdot [\mathbf{Q} + \tilde{\mathbf{N}}(\boldsymbol{\eta})] \cdot \mathbf{U} + \mathbf{B}_a \cdot \boldsymbol{\alpha} \cdot \mathbf{E}_{\text{eff}}, \quad (2.54)$$

or using (2.12) in (2.54),

$$\mathbf{E}_{\text{eff}} = \mathbf{B}_a \cdot (\mathbf{I} - \boldsymbol{\alpha} \cdot \mathbf{B}_a)^{-1} \cdot (\mathbf{Q} + \tilde{\mathbf{N}}) \cdot \mathbf{U} - (\mathbf{I} - \boldsymbol{\alpha} \cdot \mathbf{B}_a)^{-1} \cdot \mathbf{E}_{\text{mac}}. \quad (2.55)$$

Now, let \mathbf{v} be a vector defined by

$$\mathbf{v} = \mathbf{M}^{1/2} \cdot \mathbf{u}; \quad (2.56)$$

then the equations of motion can be written

$$\omega^2 \cdot \mathbf{v} = \mathbf{C}_a \cdot \mathbf{v} + \mathbf{D} \cdot \mathbf{E}_{\text{mac}}. \quad (2.57)$$

The matrices \mathbf{C}_a and \mathbf{D} are given by the following equations:

$$\mathbf{C}_a = \mathbf{C}_v + \mathbf{M}^{-1/2} (\mathbf{Q} + \tilde{\mathbf{N}}) \cdot \mathbf{B}_a \cdot (\mathbf{I} - \boldsymbol{\alpha} \cdot \mathbf{B}_a)^{-1} \times (\mathbf{Q} + \mathbf{N}) \cdot \mathbf{M}^{-1/2}, \quad (2.58)$$

$$\mathbf{D} = \mathbf{M}^{-1/2} \cdot (\mathbf{Q} + \mathbf{N}) \cdot (\mathbf{I} - \boldsymbol{\alpha} \cdot \mathbf{B}_a)^{-1}. \quad (2.59)$$

\mathbf{C}_v is the valence part of the dynamical matrix. The matrices \mathbf{C}_a and \mathbf{D} are continuous functions in the limit of vanishing wave vectors, and therefore they can be expanded in MacLaurin series of the small wave vector $\boldsymbol{\eta}$ of the reciprocal space

$$\mathbf{C}_a(\boldsymbol{\eta}) = \mathbf{C}_a(0) + i\boldsymbol{\eta} \mathbf{C}_1(0) - \frac{1}{2} \boldsymbol{\eta} \boldsymbol{\eta} \cdot \mathbf{C}_2(0) + \dots, \quad (2.60)$$

$$\mathbf{D}(\boldsymbol{\eta}) = \mathbf{D}(0) + i\boldsymbol{\eta} \mathbf{D}_1(0) - \frac{1}{2} \boldsymbol{\eta} \boldsymbol{\eta} \cdot \mathbf{D}_2(0) + \dots. \quad (2.61)$$

The matrix $\mathbf{C}_a(0)$ is singular and cannot be inverted. Nevertheless, we can define a matrix \mathbf{G} by the following relations:

$$G_{\kappa, \kappa'} = 0 \quad \text{if } \kappa \text{ or } \kappa' = 1, 2, 3 \quad (2.62)$$

$$\sum_{\kappa'} C_a(0)_{\kappa \kappa'} \cdot G_{\kappa' \kappa''} = \delta_{\kappa \kappa''}. \quad (2.63)$$

With those notations, the tensors associated with the acoustic modes can be defined by the following relations:

$$[\alpha\beta, \gamma\delta] = \frac{1}{8\pi^2 v_a} \sum_{\kappa \kappa'} (M_\kappa M_{\kappa'})^{1/2} \{ (C_2)_{\kappa \kappa'} \}_{\alpha\beta, \gamma\delta}, \quad (2.64)$$

$$(\alpha\gamma, \beta\delta) = -\frac{1}{4\pi^2 v_a} \sum_{\kappa \kappa', \kappa'' \kappa''', \mu\nu} (M_\kappa M_{\kappa'})^{1/2} \{ (G)_{\kappa'' \kappa'''} \}_{\mu\nu} \times \{ (C_1)_{\kappa \kappa'} \}_{\alpha\mu, \gamma} \{ (C_1)_{\kappa' \kappa'''} \}_{\beta\nu, \delta}, \quad (2.65)$$

$$[\beta, \alpha\gamma] = \frac{1}{2\pi v_a} \sum_{\kappa \kappa', \kappa'' \kappa''', \mu\nu} M_\kappa^{1/2} \{ (C_1)_{\kappa \kappa'} \}_{\alpha\mu, \gamma} \times \{ (G)_{\kappa'' \kappa'''} \}_{\mu\nu} \{ (D_0)_{\kappa' \kappa'''} \}_{\nu\beta} + \sum_{\kappa \kappa'} M_\kappa^{1/2} \{ (D_1)_{\kappa \kappa'} \}_{\alpha\beta, \gamma}. \quad (2.66)$$

The tensors associated with acoustic modes have been calculated by Born and Huang¹⁰ for a rigid-ion model. They obtained similar relations for the tensors $[\alpha\beta, \gamma\delta]$

TABLE I. Normal-mode frequencies for vanishing wave vectors.

Symmetry	Balkanski <i>et al.</i> ^a (cm ⁻¹)	Tell <i>et al.</i> ^b and Colbrow ^c (cm ⁻¹)	Le Toulliec ^d (cm ⁻¹)	Chosen values for the present work (cm ⁻¹)
Γ_1	305	305	298	298
Γ_6	242	235	240	240
Γ_6	256	252		256
Γ_6	85	44		44
Γ_4	211			211
Γ_4	170			170
$\Sigma_1(\text{TO})$	233.5	228	232	230
$\Sigma_1(\text{LO})$		305	302	302

^a Reference 14.

^b B. Tell, T. C. Damen, and S. P. S. Porto, Phys. Rev. **144**, 771 (1966).

^c K. Colbrow, Phys. Rev. **141**, 742 (1966).

^d R. Le Toulliec, thèse, Faculté des Sciences de l'Université de Paris, France, 1968 (unpublished).

and $(\alpha\beta, \gamma\delta)$, but our result is different for the tensor $[\alpha\beta, \gamma]$.

By a second-order development of the equations of motion for a vanishing wave vector we obtain

$$\frac{\sum_\lambda M_\lambda}{v_a} \omega^2 u_\alpha = 4\pi^2 \sum_{\beta\gamma\lambda} [\alpha\beta, \gamma\lambda] + (\alpha\gamma, \beta\lambda) q_\lambda q_\lambda u_\beta - 2\pi \sum_{\beta\gamma} [\beta, \alpha\gamma] q_\gamma E_\beta. \quad (2.67)$$

In the relation (2.67), u_α is the Cartesian component α of the displacement vector \mathbf{u} .

Elastic and Piezoelectric Tensors

The elastic and piezoelectric tensors are defined by the following relations:

$$\mathbf{S} = \mathbf{C} \cdot \mathbf{s} - \boldsymbol{\Pi} \cdot \mathbf{E}, \quad (2.68)$$

$$\mathbf{P} = \boldsymbol{\Pi} \cdot \mathbf{s} - \mathbf{a} \cdot \mathbf{E}. \quad (2.69)$$

\mathbf{S} is the strain tensor, \mathbf{s} is the stress tensor, \mathbf{a} is the static dielectric tensor, \mathbf{E} is the applied electric field, \mathbf{P} is the polarization vector, \mathbf{C} is the fourth-rank elastic tensor, and $\boldsymbol{\Pi}$ is the third-rank piezoelectric tensor.

Let a plane wave propagate in the homogeneous crystal. The displacement is given by

$$\mathbf{U} = \mathbf{U}_0 e^{2i\pi\boldsymbol{\eta} \cdot \mathbf{r} - i\omega t}. \quad (2.70)$$

The equation of motion can be written

$$\rho \frac{\partial^2 \mathbf{U}}{\partial t^2} = \text{div} \mathbf{S} \quad (2.71)$$

or

$$\rho \omega^2 \mathbf{U} = 4\pi \mathbf{c} \cdot (\boldsymbol{\eta} \boldsymbol{\eta}) \cdot \mathbf{U} + 2i\pi \boldsymbol{\Pi} \cdot \boldsymbol{\eta} \cdot \mathbf{E}. \quad (2.72)$$

By identification of Eqs. (2.67) and (2.72) and by using the symmetry properties of the tensors, we obtain the elastic and piezoelectric coefficients

$$C_{\alpha\gamma, \beta\delta} = [\alpha\beta, \gamma\delta] + [\beta\gamma, \alpha\delta] - (\beta\lambda, \alpha\gamma) - (\alpha\gamma, \beta\lambda), \quad (2.73)$$

$$\Pi_{\beta, \alpha\gamma} = [\beta, \alpha\gamma]. \quad (2.74)$$

¹¹ J. Sullivan, J. Phys. Chem. Solids **25**, 1039 (1964).

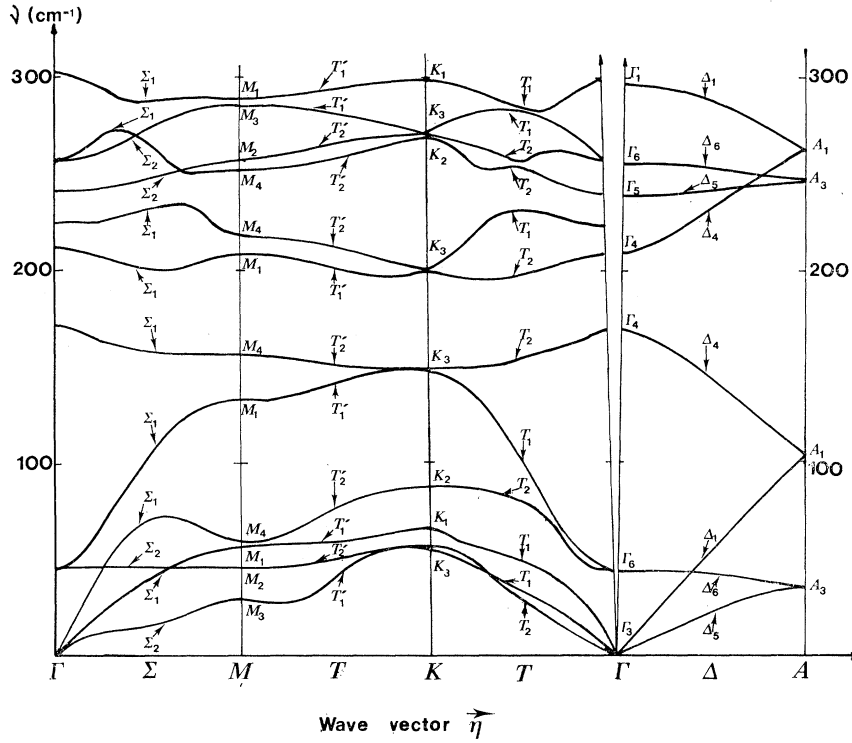


FIG. 1. Dispersion curves of the normal modes in CdS.

Symmetry properties of wurtzite require that three piezoelectric coefficients and five elastic constants only are independent and nonzero. It is possible to separate, in the expression of the elastic constants, the contribution of the internal strain. Let us use a notation similar to the one used by Sullivan.¹¹ The quantities d , e , f , g , and h are related to the internal strain and are defined by

$$d = 4\pi^2 v_a [(11,11) + (11,22)], \quad (2.75)$$

$$e = 4\pi^2 v_a (12,12), \quad (2.76)$$

$$f = 4\pi^2 v_a (33,33), \quad (2.77)$$

$$g = 4\pi^2 v_a (11,33), \quad (2.78)$$

$$h = 4\pi^2 v_a (13,13). \quad (2.79)$$

Let us also define the tensor \mathbf{P} by

$$P_{\alpha\beta,\gamma\delta} = \sum_{\kappa\kappa'} (M_{\kappa} M_{\kappa'})^{1/2} \{D_{2\kappa\kappa'}\}_{\alpha\beta,\gamma\delta}. \quad (2.80)$$

Then the five independent elastic constants can be written

$$C_{11} = P_{11,11}/8\pi^2 v_a - (d+e)/4\pi v_a, \quad (2.81)$$

$$C_{12} = (2P_{12,12} - P_{11,33})/8\pi^2 v_a - (d-e)/4\pi v_a, \quad (2.82)$$

$$C_{13} = (2P_{13,13} - P_{11,33})/8\pi^2 v_a - g/4\pi v_a, \quad (2.83)$$

$$C_{33} - P_{33,33}/8\pi^2 v_a - f/4\pi v_a, \quad (2.84)$$

$$C_{44} = P_{11,33}/8\pi^2 v_a - h/4\pi v_a. \quad (2.85)$$

¹¹ A. Manabe, A. Mitsuishi, and H. Yoshinaga, J. Appl. Phys. Japan **6**, 593 (1967).

III. CALCULATIONS AND RESULTS

Fit of Parameters

There are 11 parameters in the present model, three more than in the previous model.¹ As experimental data, we shall use the $\eta=0$ values of the optical-branch phonon frequencies. The eight frequencies so used are given in the right-hand column of Table I. We also use the experimental value of the high-frequency dielectric constant.¹¹

We proceed by giving arbitrary (trial) values to the parameters γ , $k_{r\theta}$, k_{rr} then, using Eqs. (2.24)–(2.30) and ϵ_∞ , we determine the eight parameters remaining. Then using the Eqs. (2.73) and (2.74), it is possible to calculate the eight piezoelectric and elastic constants of CdS

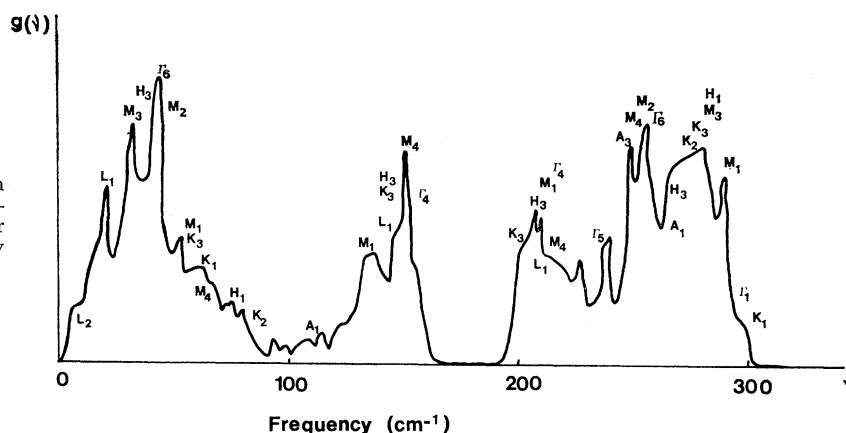
TABLE II. Force constants in CdS.

Parameter	Present work ^a (10 ⁵ dyne/cm)	Model I (10 ⁵ dyne/cm)
λ	0.9672	1.061
μ	0.2271	0.203
ν	-0.0756	-0.086
δ	-0.0255	-0.085
k_θ	-0.1780	-0.170 ^b
k_θ'	0.1944	0.154
$k_{r\theta}$	-0.0048	-0.0216
k_{rr}	0.0	missing
q^*	1.02 e	1.01 e
γ	0.03 e	missing
$(4\pi/V_a)\alpha_S$	0.589	0

^a k_{rr} has not been set equal to zero in the present work, but the least-squares method gave zero as the best value.

^b In I this constant was incorrectly given and should be of minus sign.

FIG. 2. Density of modes of vibration in CdS. The critical points due to symmetry are pointed out; others appear corresponding to points of low symmetry of the reciprocal space.



and compare them with experimental data. Those calculated values are functions of the choice of the three parameters k_{rr} , $k_{r\theta}$, γ . We have chosen those three parameters in order to minimize the sums of the squares of the differences between calculated and experimental values for the eight piezoelectric and elastic constants. Since the relation between experimental data and parameters of the model is not a linear one, the achievement of a fit between experiment and predictions is not trivial, even through 16 data were used to obtain 11 parameters. Calculations based on the shell model were unable to obtain one unique set of parameters.⁵ In Table II, the selected parameter values are listed along with values used in our earlier work for comparison. Observe that the largest changes are in the constant δ and in the three-body (angular) stiffnesses—in addition, of course, to the inclusion in the present work of the dipole deformation constants.

TABLE III. Elastic and piezoelectric constants of CdS.

Elastic constants	Measured ^a	Calculated	Internal strain
	(In units of mks)		
c_{11}	9.07	8.53	-4.30
c_{12}	5.21	4.80	1.12
c_{13}	4.64	4.52	1.43
c_{33}	9.40	9.38	-4.42
c_{44}	1.49	1.52	-1.27
	Calculated with experimental values of elastic constants ^a		
Sound velocities	(In units of m/sec)		
Wave vector $\parallel c$ axis	LA	4410	4370
	TA	1760	1800
Wave vector $\perp c$ axis	LA		4330
	TA		2000
	TA'		1760
	Present work		
Piezoelectric constants	Measured	Calculated	
	(In units of cgs)		
π_{31}	-0.245	-0.251	
π_{15}	-0.210	-0.208	
π_{33}	0.440	0.424	

^a Reference 12.

Elastic and Piezoelectric Constants

The elastic and piezoelectric constants of CdS were calculated using the values of parameters given in Table II and Eqs. (2.73) and (2.74), and the least-squares-fit procedure. Table III gives the values of the elastic and piezoelectric constants of CdS and also the contribution of internal strain to the elastic constants.

It is to be noted that the least-squares values of these macroscopic constants agree with experiment¹² to within 8% for the elastic and 3% for the piezoelectric coefficients. Computed and observed sound velocities are also given in Table III. These are an improvement over the rigid-ion (model I) results previously reported.

Normal Modes of Vibration

The eigenvalues and eigenvectors of the dynamical matrix have been calculated for 2175 different wave vectors of the reduced Brillouin zone of the reciprocal space of CdS; i.e., for 43 511 different wave vectors of the first Brillouin zone. The dispersion curves of the normal modes of vibration of CdS obtained in this way are given on Fig. 1 in the directions ΓA , ΓM , ΓK , and MK in reciprocal space.

Using the eigenfrequencies calculated for 43 511 different wave vectors of the Brillouin zone gives us the density of normal modes of vibration of CdS shown on Fig. 2. Several singularities appear in the density of modes corresponding to critical points of the reciprocal space. Some of these critical points can be obtained by symmetry considerations, and they have been indicated on Fig. 2. Several others singularities appear in the density of modes corresponding to "accidental" critical points of the reciprocal space of the crystal, which cannot be obtained by symmetry considerations. Inspecting Fig. 2, we note that a forbidden band appears in the density of modes for frequencies between 175 and 195 cm^{-1} . The density of modes can be used to determine some thermodynamical properties of CdS, such as

¹² D. Berlincourt, H. Jaffe, and L. R. Shiozawa, Phys. Rev. **129**, 1009 (1963).

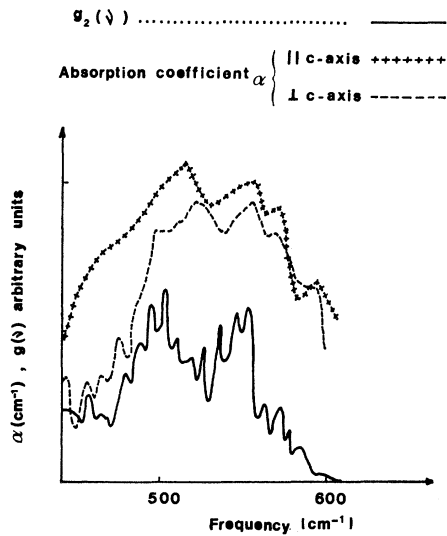


FIG. 3. Comparison between absorption coefficient and two-phonon density of modes in CdS. The calculated two-phonon density of modes shows a thinner resolution than the absorption coefficient. Indeed, our calculation was done for an harmonic approximation, where the bands are infinitely narrow.

TABLE IV. Raman-active coupled modes of vibration. Group theory shows that all the previous two-phonon combinations are Raman-active (Ref. 13).

Experimental ^a frequencies (cm ⁻¹)	Calculated frequencies (cm ⁻¹)	(Present work)
97	2Γ ₆ 2M ₂	88 94
207	M ₂ 2A ₁	204 210
328	H ₁ M ₁ K ₂ K ₃ M ₂	H ₃ M ₃ K ₃ K ₃ M ₃
347	K ₁ K ₁ H ₁ 2Γ ₄ M ₁ M ₁ M ₃ M ₁ M ₁ M ₁ K ₂	K ₂ K ₃ H ₃ 340 340 M ₁ M ₃ M ₄ M ₁ M ₄ K ₃
347	A ₁ H ₃	A ₃ H ₃
364	K ₂ K ₂ H ₁ M ₁ K ₁	K ₂ K ₃ H ₁ M ₄ K ₃
556	M ₁ 2Γ ₁ H ₁ Γ ₁	M ₂ 547 548 549 554
Σ ₁ (q → 0, LO)	Γ ₆	558
605	2Γ ₁ 2K ₁	596 600
2Σ ₁ (q → 0, LO)		604

^a B. Tell, T. C. Damen, and S. P. S. Porto, Phys. Rev. **144**, 771 (1966).

the specific heat or the Debye temperature. However, since the thermal properties are insensitive to the details of the model, we do not show the results except to remark that the calculated value of the Debye temperature at room temperature is in good agreement with experiment, and the temperature dependence $\theta(T)$ is substantially as previously given.²

Two-Phonon Density of Modes

We calculated the density of additive two-phonon modes for comparison with the observed two-phonon absorption coefficient in CdS. The absorption coefficient at frequency $\nu = \nu_1 + \nu_2$ is given by

$$d(\nu) = I_0(\nu)g_2(\nu),$$

where $I_0(\nu)$ is a factor which involves the square of the transition matrix element and is presumably slowly varying. The variation of $\alpha(\nu)$ with ν is taken to reflect the variation of $g_2(\nu)$ with ν . Since the photon momentum is taken as zero, momentum conservation requires that

$$\eta(\nu_1) + \eta(\nu_2) = 0.$$

Of course, phonons from all different branches will be included since the two-phonon selection rules are relatively weak in the Würtzite structure.¹³

Comparison of calculated $g_2(\nu)$ with experimental¹⁴ absorption coefficients are shown in Fig. 3. The location of the maximum of experimental curves and of the curve for $g_2(\nu)$ correspond, and the over-all shapes do also. The curves shown on Fig. 3 represent considerably improved agreement over that reported using the previous model (see Fig. 4 of Ref. 2). Since the variations of the double-phonon density of modes are very sensitive to the choice of a model, the correspondence between the curves of Fig. 3 is an encouraging indirect check of the validity of the model.

As shown previously, the weakness of the two-phonon selection rules in case of Raman scattering permits many two-phonon processes to be identified as producing observed peaks. The situation using the present model is the same, and a representative sampling is given in Table IV along with the revised assignments.

IV. CONCLUSION

A lattice-dynamic model including valence forces, Coulomb forces, and charge deformation has been applied to calculate the phonon dispersion in CdS and the related elastic and piezoelectric constants. The model has eleven parameters which are determined from the eight $\eta = 0$ optic-phonon frequencies and from a least-square fit to the eight macroscopic constants. Computed two-phonon density of states agrees with the observed infrared absorption in the two-phonon region.

¹³ M. A. Nusimovici, J. Phys. (Paris) **26**, 689 (1965).

¹⁴ M. Balkanski, J. M. Besson, and R. Le Toullec, in *Proceedings of the International Conference on the Physics of Semiconductors, Paris, 1964*, edited by M. Hulin (Dunod Cie, Paris, 1965), p. 1098.

Assignment of features in the observed two-phonon Raman scattering can be satisfactorily carried out using the calculated values of phonon frequencies at critical points. The model has been applied to a calculation of lattice dynamics of imperfect wurtzite lattices; results for frequencies of resonant and localized modes in a

crystal of CdS with mass substituted impurities are given in an accompanying paper.

Work applying the model to BeO, for which some experimental dispersion curves have been reported, is under way as a direct test of the model. Results and a comparison with experiment have been given elsewhere.⁵

APPENDIX

TABLE V. Lorentz matrix for vanishing wave vectors in wurtzite structure. \mathbf{B}_2 corresponds to a wave vector perpendicular to the c axis. \mathbf{B}_1 corresponds to a vanishing wave vector parallel to the c axis.

i	j	$B_{1ij}v_a$	$B_{2ij}v_a$	i	j	$B_{1ij}v_a$	$B_{2ij}v_a$
1	1	3.8012	-2.4823	3	6	-0.5632	5.7110
4	4	3.8012	-2.4823	9	12	-0.5632	5.7110
7	7	3.8012	-2.4823	1	7	-1.5063	-7.7881
10	10	3.8012	-2.4823	4	10	-1.5063	-7.7881
2	2	3.8012	3.8012	2	8	-1.5063	-1.5063
5	5	3.8012	3.8012	5	11	-1.5063	-1.5063
8	8	3.8012	3.8012	3	9	3.1126	9.2944
11	11	3.8012	3.8012	6	12	3.1126	9.2944
3	3	-7.6024	-1.3189	4	7	5.5941	-0.6918
6	6	-7.6024	-1.3189	1	10	5.5941	-0.6918
9	9	-7.6024	-1.3189	5	8	5.5941	5.5941
12	12	-7.6024	-1.3189	2	11	5.5941	5.5941
1	4	0.2866	-5.9976	6	9	-11.1882	-4.8023
7	10	0.2866	-5.9976	3	12	-11.1882	-4.8023
2	5	0.2866	0.2866				
8	11	0.2866	0.2866				

Let dipole moment

$$\mathbf{p}(l,\kappa) = \mathbf{p}_\kappa e^{i\boldsymbol{\eta} \cdot \mathbf{R}_l} \quad (\text{A1})$$

be at the site of ion (l,κ) , then the field at ion $(0,\kappa')$ can be expressed by

$$\mathbf{E}_{\kappa'} = \mathbf{B}_{\kappa\kappa'}(\boldsymbol{\eta}) \mathbf{P}_\kappa. \quad (\text{A2})$$

The matrix $\mathbf{B}(\boldsymbol{\eta})$ composed of the blocks $\mathbf{B}_{\kappa\kappa'}(\boldsymbol{\eta})$ defined by (A2) is the Lorentz matrix. This matrix is discontinuous for $\boldsymbol{\eta} \rightarrow 0$, and it has two limits $\mathbf{B}_1(0)$ and $\mathbf{B}_2(0)$ if $\boldsymbol{\eta}$ goes, respectively, to zero parallel or perpendicular to the crystal c axis. The elements of $\mathbf{B}_1(0)$ and $\mathbf{B}_2(0)$ have been computed and are given in Table V.

Vibrations of a Mass Defect in Cadmium Sulfide†

MICHEL A. NUSIMOVICI*‡ AND MINKO BALKANSKI

*Laboratoire de Physique des Solides de la Faculté des Sciences de Paris, France,
Equipe de Recherche associée au Centre National de la Recherche Scientifique*

AND

JOSEPH L. BIRMAN*

Physics Department, New York University, New York, New York

(Received 19 May 1969)

A Green's-function technique is used to study the vibrations of a substitutional impurity in CdS. Three cases have been investigated, corresponding to localized modes, gap modes, and in-band resonant modes. The theoretical results are in close agreement with experimental results for the gap mode of vibration of a Se impurity substituted for the S ion and the resonant mode of a Mn impurity substituted for the Cd ion in CdS.

I. INTRODUCTION AND METHOD

WE have calculated the frequency spectrum of the vibrations of an imperfect CdS (wurtzite)

† Paper based in part on the thesis presented to the Faculté des Sciences, University of Paris, Paris, France, for the degree Docteur-ès-Sciences Physiques, 1968 by Michel A. Nusimovici.

crystal containing isolated substitutional mass defects at the Cd or S site. We have used the results of our

* Supported in part by the Aerospace Research Laboratories, Wright-Patterson Air Force Base, Dayton, Ohio, and the U. S. Army Research Office, Durham, N. C.

‡ Permanent address: Laboratoire de Physique des Solides, Faculté des Sciences, 35-Rennes, France.